explained in the Discussion section. After this mapping process, we gathered multiple reads into one read based on the mapping information of the 5'-end of each read in order to remove sequence duplication.

In this analysis, we defined the regions that contained origins for both sense and antisense transcripts as bidirectionally transcribed regions. Based on our transcript mapping and reference gene information, we adjusted the genomic locations of TSSs. For this purpose, we identified the transcript-enriched regions using MACS software under the non-MACS model (--nomodel; v.1.4.1) [33]. In this analysis, minimum FDR cutoff for peak detection is 0.05. We defined the 5'-ends of these regions as the adjusted TSS when the 5'-ends were located from −1,000 bp to +1,000 bp from the reference TSS. In drawing the distribution of sense and antisense mapped reads around TSSs, we eliminated the furthest-upstream reads composing the transcript-enriched regions because these reads were utilized for the adjustment of the genomic location of TSSs that resulted in the intentional overrepresentation of read enrichment at the TSSs.

For the efficient calculation of density of the ratio of sense mapped reads to antisense mapped reads, genomic locations every 100 bp were first extracted, and then filtered based on the criteria that more than one sense mapped read and antisense mapped read existed in order to pick up the genomic fragments in which both strands were actively utilized. The 100-bp fragments starting from the representative genomic locations were further screened based on the criterion that the total length of the sense or antisense mapped reads was more than 300 bp.

RT-PCR analysis

To examine RNA expression, total RNA isolated from tissues with TRIzol reagent (Life Technologies Co.) was treated with DNase I (Life Technologies Co.) and reverse-transcribed with each respective gene-specific primer or oligo-dT primer using the SuperScriptIII First-Strand Synthesis System (Life Technologies Co.). Strand-specific PCR was carried out with specific primers for each transcript (see Additional file 1: Table S9).

Quantitative PCR was performed with KAPA SYBR Fast qPCR Kit (KAPA Biosystems) using an Applied Biosystems StepOnePlus Real-Time PCR System (Life Technologies Co.). Quantitative PCR was carried out with specific primers for each transcript (see Additional file 1: Table S11). Relative quantities of mRNA were normalized by the glyceraldehyde-3-phosphate dehydrogenase (*Gapdh*) mRNA content.

RNA quantification and the identification of candidates for bidirectional promoter regions

To quantify the transcription level around TSSs based on directional RNA-seq data, we counted the number of mapped reads in the region from −1,000 bp to +1,000 bp relative to the TSS and normalized this number by RPKM. In order to focus on the promoter regions where ncRNA is transcribed, we removed the promoter regions where two mRNAs were transcribed in a HtH manner from promoters of protein-coding genes with Ensembl Gene ID (NCBIM37 for the mouse genome and GRCh37 for the human genome) available from Ensembl Genes Database [34]. Cufflinks (v2.1.1) was used with default parameters for quantification of RPKM of known protein-coding genes [35].

We utilized the MACS output file, which contains the location of transcript-enriched regions. We sorted the transcript-enriched regions according to the genomic location. If a minus transcript was located next to a plus transcript, we regarded their boundary sequence as the target for further analysis of the genomic properties driving bidirectional transcription. We narrowed down the candidates based on the minus-plus pitch. We only analyzed the minus-plus pitches that were mutually located within 2,000 bp.

Calculation of ORF length

To examine the length of ORFs, we used EMBOSS: getorf [36] with the sequences of the downstream region (+1 to +1,000 bp) and of the upstream region (−1,000 to −1 bp) of the candidate pancRNA-bearing genes. In this analysis, we defined an ORF as a region which begins with a START codon and ends with a STOP codon.

De novo motif discovery

For motif discovery, we employed the rGADEM package (v.1.0.1) [37], which is available through Bioconductor [38], with the default parameter (P-value < 0.0002) [39] with DNA sequences from −1,000 bp to +1,000 bp relative to TSSs of the candidate pancRNA-bearing genes. We calculated the observed frequencies of "CCGCCG" or "CGGCGG" sequences from −1,000 bp to +1,000 bp relative to TSSs of the candidate pancRNA-bearing genes with sliding window of width 100 bp. The average numbers of "CCGCCG" and "CGGCGG" found in a sequence were plotted with a sliding window of width 100 bp.

Additional files

Additional file 1: Table S1. Summary of directional RNA sequencing. **Table S2.** Comparison of the number of the uniquely mapped reads in directional RNAseq data of chimpanzee samples mapped onto the human versus the chimpanzee genome. **Table S3.** The percentage of transcribed regions in the whole genome in various chimpanzee tissues. **Table S4.** RPKM of the upstream and downstream regions of TSSs of genes belonging to each subgroup in each indicated tissue. **Table S5.** RPKM of the upstream and downstream regions of TSSs of genes with tissuespecific pancRNAs in various tissues. **Table S6.** Pearson correlation coefficient between the expression level of pancRNA and the corresponding mRNA. **Table S7.** The bias of the

pancRNA-bearing protein-coding genes for CpG islands in various chimpanzee tissues. **Table S8.** The percentage of genes expressed in various chimpanzee tissues with both "CCGCCG" and "CGGCGG" sequences. **Table S9.** Primers for strand-specific RT-PCR analysis. **Table S10.** shRNA sequences. **Table S11.** Primers for quantitative RT-PCR analysis.

Additional file 2: Figure S1. The depth of coverage of each base in the mouse genome with reads from directional RNAseq data of the mouse cerebral cortex. **Figure S2.** Either top or bottom strand of genome is preferentially utilized for transcription. **Figure S3.** Density plots of the ratio of top strand-mapped reads to bottom strand-mapped reads. **Figure S4.** The distribution of sense and antisense mapped reads around the TSS of each gene fraction in the mouse cerebellum, mouse heart, chimpanzee cerebral cortex, and chimpanzee cerebellum. **Figure S5.** The distribution of longest ORFs in downstream region and upstream region. **Figure S6.** The Average RPKM of genes bearing pancRNAs with the 100 top-ranked RPKM and those with the bottom-ranked RPKM relative to RPKM of total genes in all samples. **Figure S7.** Expression of pancRNAs was accompanied by that of corresponding mRNAs in a tissue-specific manner. **Figure S8.** Sequence characteristics of pancRNA-bearing genes in the mouse cerebellum, mouse heart, chimpanzee cerebral cortex and chimpanzee cerebellum.

Abbreviations

ncRNA: Non-coding RNA; TSS: Transcription start site; pancRNA: Promoter-associated ncRNA; SAT: Sense-antisense transcript; lncRNA: Long intergenic non-coding RNA; CGI: CpG island; HtH: Head-to-head; RPKM: Reads per kilobase per million mapped reads; ORF: Open reading frame.

Competing interests

The authors declare that they have no competing interests.

Authors' contributions

MU conceived the project, designed and performed experiments, conducted bioinformatic analysis and drafted the manuscript. ON conducted bioinformatic analysis. YG contributed to the sample preparation for directional RNA-seq. KN designed experiments and drafted the manuscript. KA designed experiments and drafted the manuscript. TI conceived the project, designed experiments, conducted bioinformatic analysis, coordinated the study and drafted the manuscript. All authors read and approved the final manuscript.

Acknowledgements

We thank the Great Ape Information Network (GAIN) and Kumamoto Sanctuary, Wildlife Research Center, Kyoto University for chimpanzee samples. We thank Atsushi Toyoda and Yutaka Suzuki for directional RNA sequencing, Takao Oishi and Hiroo Imai for primate sample preparation, Koichiro Irie and Hideyuki Nakashima for primary culture of murine cortical neuron, and Nobuhiko Hamazaki, Naoki Yamamoto, Naoyuki Fuse, Itoshi Nikaido, Hiroki Danno and Hiroki Ueda for useful discussions on directional RNA-seq analyses. We thank the National Institute of Genetics (NIG) and the Graduate School of Frontier Sciences in the University of Tokyo for technical assistance. We thank Elizabeth Nakajima for proofreading the manuscript. This work was supported in part by Grant-in-aid Nos. 21688021 and 24380158 (to T. I.), Global COE program A06 (to Kyoto University), the Grants to Excellent Graduate Schools (MEXT) program of Kyoto University, Grant-in-aid No. 221S0002 for Scientific Research on Innovative Areas "Genome Science" from the Ministry of Education, Culture, Sports, Science and Technology of Japan, and by the Asahi Glass Foundation (to T. I.), and a Research Fellowship of the Japan Society for the Promotion of Science for Young Scientists (M.U.).

Author details

[1]Department of Biophysics and Global COE Program, Graduate School of Science, Kyoto University, Kitashirakawa-Oiwake, Sakyo-ku, Kyoto 606-8502, Japan. [2]Department of Stem Cell Biology and Medicine, Graduate School of Medical Sciences, Kyushu University, 3-1-1 Maidashi, Higashi-ku, Fukuoka 812-8581, Japan. [3]Genome Resource and Analysis Unit, RIKEN Center for Developmental Biology, 2-2-3 Minatojima-Minamimachi, Chuo-ku, Kobe 650-0047, Japan. [4]Department of Cellular and Molecular Biology, Primate Research Institute, Kyoto University, 41-2 Kanrin, Inuyama, Aichi 484-8506, Japan. [5]Present address: Department of Brain Sciences, Center for Novel Science Initiatives, National Institutes of Natural Sciences, 38 Nishigonaka Myodaiji, Okazaki, Aichi 444-8585, Japan.

Received: 16 June 2013 Accepted: 15 January 2014
Published: 17 January 2014

References

1. Lander ES, Linton LM, Birren B, Nusbaum C, Zody MC, Baldwin J, Devon K, Dewar K, Doyle M, FitzHugh W, Funke R, Gage D, Harris K, Heaford A, Howland J, Kann L, Lehoczky J, LeVine R, McEwan P, McKernan K, Meldrim J, Mesirov JP, Miranda C, Morris W, Naylor J, Raymond C, Rosetti M, Santos R, Sheridan A, Sougnez C, *et al*: **Initial sequencing and analysis of the human genome.** *Nature* 2001, **409**:860–921.
2. Carninci P, Kasukawa T, Katayama S, Gough J, Frith MC, Maeda N, Oyama R, Ravasi T, Lenhard B, Wells C, Kodzius R, Shimokawa K, Bajic VB, Brenner SE, Batalov S, Forrest AR, Zavolan M, Davis MJ, Wilming LG, Aidinis V, Allen JE, Ambesi-Impiombato A, Apweiler R, Aturaliya RN, Bailey TL, Bansal M, Baxter L, Beisel KW, Bersano T, Bono H, *et al*: **The transcriptional landscape of the mammalian genome.** *Science* 2005, **309**:1559–1563.
3. The ENCODE Project Consortium: **An integrated encyclopedia of DNA elements in the human genome.** *Nature* 2012, **489**:57–74.
4. Moazed D: **Small RNAs in transcriptional gene silencing and genome defence.** *Nature* 2009, **457**:413–420.
5. Siomi H, Siomi MC: **On the road to reading the RNA-interference code.** *Nature* 2009, **457**:396–404.
6. Wagner RW, Smith JE, Cooperman BS, Nishikura K: **A double-stranded RNA unwinding activity introduces structural alterations by means of adenosine to inosine conversions in mammalian cells and Xenopus eggs.** *Proc Natl Acad Sci USA* 1989, **86**:2647–2651.
7. Beltran M, Puig I, Peña C, García JM, Alvarez AB, Peña R, Bonilla F, de Herreros AG: **A natural antisense transcript regulates Zeb2/Sip1 gene expression during Snail1-induced epithelial-mesenchymal transition.** *Genes Dev* 2008, **22**:756–769.
8. Munroe SH, Lazar MA: **Inhibition of c-erbA mRNA splicing by a naturally occurring antisense RNA.** *J Biol Chem* 1991, **266**:22083–22086.
9. Kimelman D, Kirschner MW: **An antisense mRNA directs the covalent modification of the transcript encoding fibroblast growth factor in Xenopus oocytes.** *Cell* 1989, **59**:687–696.
10. Hastings ML, Ingle HA, Lazar MA, Munroe SH: **Post-transcriptional regulation of thyroid hormone receptor expression by cis-acting sequences and a naturally occurring antisense RNA.** *J Biol Chem* 2000, **275**:11507–11513.
11. Ebralidze AK, Guibal FC, Steidl U, Zhang P, Lee S, Bartholdy B, Jorda MA, Petkova V, Rosenbauer F, Huang G, Dayaram T, Klupp J, O'Brien KB, Will B, Hoogenkamp M, Borden KLB, Bonifer C, Tenen DG: **PU.1 expression is modulated by the balance of functional sense and antisense RNAs regulated by a shared cis-regulatory element.** *Genes Dev* 2008, **22**:2085–2092.
12. Spigoni G, Gedressi C, Mallamaci A: **Regulation of Emx2 expression by antisense transcripts in murine cortico-cerebral precursors.** *PLoS One* 2010, **5**:e8658.
13. Carrieri C, Cimatti L, Biagioli M, Beugnet A, Zucchelli S, Fedele S, Pesce E, Ferrer I, Collavin L, Santoro C, Forrest ARR, Carninci P, Biffo S, Stupka E, Gustincich S: **Long non-coding antisense RNA controls *Uchl1* translation through an embedded SINEB2 repeat.** *Nature* 2012, **491**:454–457.
14. Katayama S, Tomaru Y, Kasukawa T, Waki K, Nakanishi M, Nakamura M, Nishida H, Yap CC, Suzuki M, Kawai J, Suzuki H, Carninci P, Hayashizaki Y, Wells C, Frith M, Ravasi T, Pang KC, Hallinan J, Mattick J, Hume DA, Lipovich L, Batalov S, Engstrom PG, Mizuno Y, Faghihi MA, Sandelin A, Chalk AM, Mottagui-Tabar S, Liang Z, Lenhard B, *et al*: **Antisense Transcription in the Mammalian Transcriptome.** *Science* 2005, **309**:1564–1566.
15. Ambros V: **The functions of animal microRNAs.** *Nature* 2004, **431**:350–355.
16. Matzke MA, Birchler JA: **RNAi-mediated pathways in the nucleus.** *Nat Rev Genet* 2005, **6**:24–35.
17. Fukagawa T, Nogami M, Yoshikawa M, Ikeno M, Okazaki T, Takami Y, Nakayama T, Oshimura M: **Dicer is essential for formation of the heterochromatin structure in vertebrate cells.** *Nat Cell Biol* 2004, **6**:784–791.
18. Morris KV, Chan SW-L, Jacobsen SE, Looney DJ: **Small interfering RNA-induced transcriptional gene silencing in human cells.** *Science* 2004, **305**:1289–1292.

19. Wang KC, Yang YW, Liu B, Sanyal A, Corces-Zimmerman R, Chen Y, Lajoie BR, Protacio A, Flynn RA, Gupta RA, Wysocka J, Lei M, Dekker J, Helms JA, Chang HY: **A long noncoding RNA maintains active chromatin to coordinate homeotic gene expression.** *Nature* 2011, **472**:120–124.
20. Cabianca DS, Casa V, Bodega B, Xynos A, Ginelli E, Tanaka Y, Gabellini D: **A Long ncRNA links copy number variation to a polycomb/trithorax epigenetic switch in FSHD muscular dystrophy.** *Cell* 2012, **149**:819–831.
21. Antequera F: **Structure, function and evolution of CpG island promoters.** *Cell Mol Life Sci* 2003, **60**:1647–1658.
22. Lavia P, Macleod D, Bird A: **Coincident start sites for divergent transcripts at a randomly selected CpG-rich island of mouse.** *EMBO J* 1987, **6**:2773–2779.
23. Imamura T, Yamamoto S, Ohgane J, Hattori N, Tanaka S, Shiota K: **Non-coding RNA directed DNA demethylation of Sphk1 CpG island.** *Biochem Biophys Res Commun* 2004, **322**:593–600.
24. Tomikawa J, Shimokawa H, Uesaka M, Yamamoto N, Mori Y, Tsukamura H, Maeda K, Imamura T: **Single-stranded noncoding RNAs mediate local epigenetic alterations at gene promoters in rat cell lines.** *J Biol Chem* 2011, **286**:34788–34799.
25. Djebali S, Davis CA, Merkel A, Dobin A, Lassmann T, Mortazavi A, Tanzer A, Lagarde J, Lin W, Schlesinger F, Xue C, Marinov GK, Khatun J, Williams BA, Zaleski C, Rozowsky J, Röder M, Kokocinski F, Abdelhamid RF, Alioto T, Antoshechkin I, Baer MT, Bar NS, Batut P, Bell K, Bell I, Chakrabortty S, Chen X, Chrast J, Curado J, *et al*: **Landscape of transcription in human cells.** *Nature* 2012, **489**:101–108.
26. Marchler-Bauer A, Lu S, Anderson JB, Chitsaz F, Derbyshire MK, DeWeese-Scott C, Fong JH, Geer LY, Geer RC, Gonzales NR, Gwadz M, Hurwitz DI, Jackson JD, Ke Z, Lanczycki CJ, Lu F, Marchler GH, Mullokandov M, Omelchenko MV, Robertson CL, Song JS, Thanki N, Yamashita RA, Zhang D, Zhang N, Zheng C, Bryant SH: **CDD: a Conserved Domain Database for the functional annotation of proteins.** *Nucleic Acids Res* 2011, **39**:D225–D229.
27. Barrett T, Wilhite SE, Ledoux P, Evangelista C, Kim IF, Tomashevsky M, Marshall KA, Phillippy KH, Sherman PM, Holko M, Yefanov A, Lee H, Zhang N, Robertson CL, Serova N, Davis S, Soboleva A: **NCBI GEO: archive for functional genomics data sets–update.** *Nucleic Acids Res* 2013, **41**:D991–D995.
28. Shen Y, Yue F, McCleary DF, Ye Z, Edsall L, Kuan S, Wagner U, Dixon J, Lee L, Lobanenkov VV, Ren B: **A map of the cis-regulatory sequences in the mouse genome.** *Nature* 2012, **488**:116–120.
29. Gardiner-Garden M, Frommer M: **CpG islands in vertebrate genomes.** *J Mol Biol* 1987, **196**:261–282.
30. Derrien T, Johnson R, Bussotti G, Tanzer A, Djebali S, Tilgner H, Guernec G, Martin D, Merkel A, Knowles DG, Lagarde J, Veeravalli L, Ruan X, Ruan Y, Lassmann T, Carninci P, Brown JB, Lipovich L, Gonzalez JM, Thomas M, Davis CA, Shiekhattar R, Gingeras TR, Hubbard TJ, Notredame C, Harrow J, Guigo R: **The GENCODE v7 catalog of human long noncoding RNAs: analysis of their gene structure, evolution, and expression.** *Genome Res* 2012, **22**:1775–1789.
31. Ginno PA, Lott PL, Christensen HC, Korf I, Chédin F: **R-loop formation is a distinctive characteristic of unmethylated human CpG island promoters.** *Mol Cell* 2012, **45**:814–825.
32. Trapnell C, Pachter L, Salzberg SL: **TopHat: discovering splice junctions with RNA-Seq.** *Bioinformatics* 2009, **25**:1105–1111.
33. Zhang Y, Liu T, Meyer CA, Eeckhoute J, Johnson DS, Bernstein BE, Nusbaum C, Myers RM, Brown M, Li W, Liu XS: **Model-based Analysis of ChIP-Seq (MACS).** *Genome Biol* 2008, **9**:R137.
34. Flicek P, Amode MR, Barrell D, Beal K, Brent S, Carvalho-Silva D, Clapham P, Coates G, Fairley S, Fitzgerald S, Gil L, Gordon L, Hendrix M, Hourlier T, Johnson N, Kahari AK, Keefe D, Keenan S, Kinsella R, Komorowska M, Koscielny G, Kulesha E, Larsson P, Longden I, McLaren W, Muffato M, Overduin B, Pignatelli M, Pritchard B, Riat HS, *et al*: **Ensembl 2012.** *Nucleic Acids Res* 2011, **40**:D84–D90.
35. Trapnell C, Williams BA, Pertea G, Mortazavi A, Kwan G, van Baren MJ, Salzberg SL, Wold BJ, Pachter L: **Transcript assembly and quantification by RNA-Seq reveals unannotated transcripts and isoform switching during cell differentiation.** *Nat Biotechnol* 2010, **28**:511–515.
36. Rice P, Longden I, Bleasby A: **EMBOSS: the European molecular biology open software suite.** *Trends Genet* 2000, **16**:276–277.
37. **rGADEM: de novo motif discovery (R package version 2.8.0).** [http://www.bioconductor.org/packages/release/bioc/html/rGADEM.html]
38. Gentleman RC, Carey VJ, Bates DM, Bolstad B, Dettling M, Dudoit S, Ellis B, Gautier L, Ge Y, Gentry J, Hornik K, Hothorn T, Huber W, Iacus S, Irizarry R, Leisch F, Li C, Maechler M, Rossini AJ, Sawitzki G, Smith C, Smyth G, Tierney L, Yang JYH, Zhang J: **Bioconductor: open software development for computational biology and bioinformatics.** *Genome Biol* 2004, **5**:R80.
39. Li L: **GADEM: a genetic algorithm guided formation of spaced dyads coupled with an EM algorithm for motif discovery.** *J Comput Biol* 2009, **16**:317–329.

doi:10.1186/1471-2164-15-35
Cite this article as: Uesaka *et al.*: Bidirectional promoters are the major source of gene activation-associated non-coding RNAs in mammals. *BMC Genomics* 2014 **15**:35.

Neurobiology of Disease 49 (2013) 29–40

Contents lists available at SciVerse ScienceDirect

Neurobiology of Disease

journal homepage: www.elsevier.com/locate/ynbdi

Mouse with $Na_v1.1$ haploinsufficiency, a model for Dravet syndrome, exhibits lowered sociability and learning impairment

Susumu Ito [a,b,1], Ikuo Ogiwara [a,1], Kazuyuki Yamada [c], Hiroyuki Miyamoto [d,e], Takao K. Hensch [d,f,g], Makiko Osawa [b], Kazuhiro Yamakawa [a,*]

[a] Laboratory for Neurogenetics, RIKEN Brain Science Institute, 2-1 Hirosawa, Wako, Saitama 351-0198, Japan
[b] Department of Pediatrics, Graduate School of Medicine, Tokyo Women's Medical University, 8-1 Kawada-cho, Shinjuku, Tokyo 162-8666, Japan
[c] Laboratory for Support Unit for Animal Resources Development, RIKEN Brain Science Institute, 2-1 Hirosawa, Wako, Saitama 351-0198, Japan
[d] Laboratory for Neuronal Circuit Development, RIKEN Brain Science Institute, 2-1 Hirosawa, Wako, Saitama 351-0198, Japan
[e] PRESTO, JST, 4-1-8 Honcho, Kawaguchi, Saitama 332-0012, Japan
[f] Department of Molecular and Cellular Biology and Center for Brain Science, Harvard University, Northwest Building, 52 Oxford Street, NW 347.10, Cambridge, MA 02138, USA
[g] Department of Neurology, FM Kirby Neurobiology Center, Children's Hospital Boston, Harvard Medical School, 320 Longwood Ave, CLS 13036, Boston, MA 02115, USA

ARTICLE INFO

Article history:
Received 13 March 2012
Revised 26 July 2012
Accepted 4 August 2012
Available online 16 August 2012

Keywords:
SCN1A
Lowered sociability
Spatial learning deficit
Parvalbumin
Interneuron

ABSTRACT

Dravet syndrome is an intractable epileptic encephalopathy characterized by early onset epileptic seizures followed by cognitive decline, hyperactivity, autistic behaviors and ataxia. Most Dravet syndrome patients possess heterozygous mutations of *SCN1A* gene encoding voltage-gated sodium channel α_1 subunit ($Na_v1.1$). We have previously reported that mice heterozygous for a nonsense mutation in *Scn1a* developed early onset epileptic seizures. However, the learning ability and sociability of the mice remained to be investigated. In the present study, we subjected heterozygous *Scn1a* mice to a comprehensive behavioral test battery. We found that while heterozygous *Scn1a* mice had lowered spontaneous motor activity in home cage, they were hyperactive in novel environments. Moreover, the mice had low sociability and poor spatial learning ability that correspond to the autistic behaviors and cognitive decline seen in Dravet syndrome patients. These results suggest that $Na_v1.1$ haploinsufficiency intrinsically contributes to not only epileptic seizures but also lowered sociability and learning impairment in heterozygous *Scn1a* mutant mice, as it should also be the case in patients with Dravet syndrome.

Introduction

Dravet syndrome, alternatively known as severe myoclonic epilepsy in infancy (SMEI; OMIM ID: 607208), is an intractable epileptic encephalopathy mainly caused by heterozygous mutations of *SCN1A* gene encoding voltage-gated sodium channel α_1 subunit $Na_v1.1$ (Claes et al., 2001; Depienne et al., 2009; Fujiwara et al., 2003; Harkin et al., 2007; Nakayama et al., 2010; Sugawara et al., 2002). Recurrent intractable seizures first appear in children aged less than one year, who otherwise develop normally before disease onset (Dravet et al., 2005). Cognitive decline, ataxia, hyperactivity and autistic behaviors including poor social relationships and gestural stereotypy generally accompany recurrent seizures (Caraballo and Fejerman, 2006; Cassé-Perrot et al., 2001; Dravet et al., 2005; Nolan et al., 2006; Ragona et al., 2010; Wolff et al., 2006). Heterozygous *SCN1A* mutations have also been described in patients with milder epilepsies including generalized epilepsy with febrile seizures plus (GEFS+; OMIM ID: 604233) (Escayg et al., 2000; Sugawara et al., 2001). While patients with these mild seizure disorders normally do not develop significant psychiatric conditions, we recently reported that familial cases of GEFS+ in those patients showed wide phenotypic variation including panic disorder and Asperger's syndrome (Osaka et al., 2007). Rare *SCN1A* variants have also been reported in some autism families and a patient with sporadic idiopathic autism (O'Roak et al., 2011; Weiss et al., 2003). We and other researchers recently reported that *Scn1a* mutant mice, as models for Dravet syndrome, showed epileptic seizures (Ogiwara et al., 2007; Yu et al., 2006). However, the learning ability and sociability of *Scn1a* mutant mice remained to be investigated.

In this study, we found that mice heterozygous for a nonsense *Scn1a* mutation (Ogiwara et al., 2007) had lowered sociability and poor spatial learning ability, those should be relevant to the clinical features of Dravet syndrome. These results suggest that $Na_v1.1$ haploinsufficiency causes autistic behaviors and cognitive decline in addition to epileptic seizures in heterozygous *Scn1a* mutant mice as well as in patients with Dravet syndrome.

* Corresponding author. Fax: +81 48 467 7095.
E-mail address: yamakawa@brain.riken.jp (K. Yamakawa).
[1] Equal contribution.
Available online on ScienceDirect (www.sciencedirect.com).

0969-9961/$ – see front matter © 2012 Elsevier Inc. All rights reserved.
http://dx.doi.org/10.1016/j.nbd.2012.08.003

Materials and methods

Mice

Mice were handled in accordance with the guidelines of the Animal Experiment Committee of RIKEN Brain Science Institute. Heterozygous mice (*Scn1a*$^{RX/+}$) carrying a nonsense mutation in *Scn1a*, R1407X, were described previously (Ogiwara et al., 2007). The mice were backcrossed for 10 generations onto a C57BL/6J background from an initial 129 background. We preferred mice on the C57BL/6J background instead of the 129 background for the three-chambered social interaction test because 129 mice have innate low levels of social behavior in this test (Moy et al., 2007). The neomycin cassette was removed from the mutated allele by crossing a backcross generation N5 mouse with a CAG-FLPe deleter mouse with a C57BL/6J background (Kanki et al., 2006). Food and water were available ad libitum, and cages were kept at 23 ± 2 °C and 55 ± 10% humidity on a 12-hour light/dark cycle with the lights off at 20:00. All mice were housed in groups of four mice (2 *Scn1a*$^{RX/+}$ and 2 *Scn1a*$^{+/+}$ mice) per cage until used in behavioral tests. All tests except for the home cage spontaneous activity test were conducted in the morning during the light phase of the light/dark cycle. The mice were habituated to the behavioral testing room for at least 30 min before the beginning of each experiment. N10 *Scn1a*$^{RX/+}$ male mice and age-matched wild-type (*Scn1a*$^{+/+}$) male littermates (n = 12, each group) were tested on a battery of tests in the following order: the home cage spontaneous activity test, the open field test, the three-chambered social interaction test, the elevated-plus maze test, the Barnes maze test, the light/dark box test, the free-moving social test, and the electroencephalography (EEG) recordings. All tests were performed in the same order and with at least one week interval. Furthermore, the buried food test was performed using N13 *Scn1a*$^{RX/+}$ male mice and age-matched *Scn1a*$^{+/+}$ male littermates (n = 11, each group), and the rotarod test and the footprint test were performed using N14 *Scn1a*$^{RX/+}$ male mice and age-matched *Scn1a*$^{+/+}$ male littermates (n = 8, each group). The behavioral tests were performed blindly.

Scn1a$^{RX/+}$ mice on the C57BL/6J background generally develop spontaneous generalized seizures at an age of ~16 days (Cao et al., 2012; Ogiwara et al., 2007). Spontaneous seizures occur frequently between the third and fourth postnatal weeks. During this period, some mice suffer sudden death immediately after having seizures or die of emaciation. In the sixth postnatal week, the frequencies of spontaneous seizures and the risk of sudden death following seizures decrease. The behavioral tests were started between the eighth and tenth postnatal weeks, after the peak period of spontaneous seizures and sporadic sudden death. The *Scn1a*$^{RX/+}$ mice employed in this study showed no seizures at least during the behavioral tests.

Home cage spontaneous activity test

The home cage spontaneous activity test was performed as previously described (Steele et al., 2007). Eight- to 10-week-old male mice were housed individually in cages (19 × 26 × 12.5 cm) and left to become habituated to the cages under a 12-hour light/dark cycle (lights off at 20:00) with access to food and water ad libitum for 6 days. Behaviors were video recorded during the night time (12 h) on day 7, assigned by the HomeCageScan system (Clever Sys, Reston, VA), and classified into nine behavioral types consisting of 'walking', 'rearing', 'hanging', 'grooming', 'eating', 'drinking', 'resting', 'micromovements' and 'unclassified', as previously described (Jhuang et al., 2010). The accuracy rate of the automatic annotation system against human observers was estimated to be ~60%, while the inter-human observer concordance rate was ~70% (Jhuang et al., 2010). Walking was further divided into three subtypes including 'walking fast', 'turning' and 'walking slowly'. Measurements of distance traveled and time spent walking, walking fast, turning, walking slowly, rearing, hanging, grooming, eating, drinking, resting and making micromovements of the head were made.

Open field test

Exploratory activities of 10- to 12-week-old male mice in a novel open field (60 × 60 × 40 cm) were analyzed every 10 min during a period of 30 min using Image J OF software (O'Hara & Co., Tokyo, Japan). Measurements of total distance traveled and time spent in the center of the open field (area > 12 cm from the walls) were made.

Three-chambered social interaction test

The social behavior apparatus was a modified three-chambered apparatus with a video recording system (Moy et al., 2007; Silverman et al., 2010). The apparatus was a rectangular, three-chambered box (60 × 42 × 22 cm) made from clear acrylic plates. Two partitions divided the box into three identical 20-cm-long chambers. Square openings (10 × 10 cm) in the bottom of the partitions allowed mice to move among the three chambers. Ten-centimeter column wire cages with 3-mm grid mesh were used to enclose stranger mice, which were 7- to 8-week-old male C57BL/6J mice that had been habituated to placement in the same small cage for 20 min per day for 3 days before the test. The social behavior test was performed as described previously (Moy et al., 2007). A 15- to 16-week-old male mouse was placed in the center chamber of the three-chambered box and allowed to explore the entire test box for 10 min for habituation. Each of the side chambers contained an empty wire cage. After the habituation period, the mouse was put in the center chamber, an unfamiliar mouse (stranger 1) was enclosed in a wire cage in one of the side chambers, and an empty wire cage was placed in the opposite side chamber. Then, the test mouse was allowed to explore the entire test box for 10 min (the test for sociability). At the end of the 10-minute session, a novel unfamiliar mouse (stranger 2) was placed in the empty wire cage. The test mouse was again allowed to explore the entire test box for another 10 min (the test for preference for social novelty). Videos were analyzed to determine the time spent in each chamber and time spent sniffing each wire cage.

Elevated-plus maze test

The elevated-plus maze consisted of two orthogonal closed and open arms (25 cm long) forming a cross, with a quadrangular area located at the intersection. The arms and quadrangular area were made of white acrylic and were elevated 60 cm above the floor. The walls of the closed arms were made of transparent acrylic. A 19-week-old male mouse was placed in the center section and allowed to explore the maze freely for 5 min; activities were analyzed using Image J EPM software (O'Hara & Co.). Measurements of distance traveled, time spent in the open and closed arms and center field and number of entries into the open and closed arms were made.

Barnes maze test

The Barnes maze test was performed as previously described (Pompl et al., 1999). The maze consisted of a white circular platform with 12 circular holes and was affixed 60 cm above the floor (O'Hara & Co). A black plastic escape box (17 × 13 × 7 cm) was located under one of the holes numbered 1, 4, 7 and 10. The hole above the escape box represented the target. One day before the beginning of training (day 0), each 20- to 22-week-old male mouse was allowed to explore the maze without the escape box for 5 min and then placed into an escape box, which was placed underneath the target hole during acquisition training and reversal training performed later, for habituation. On days 1–4 (acquisition days a1–a4), acquisition training took place with three trials per day. In each trial, the mouse was placed in a

center column for 10 s and then allowed to find and enter the target hole with the escape box for 5 min. The mouse was allowed to remain in the box for 60 s, regardless of whether it found the target hole. The location of the target hole was consistent for a given mouse but randomized across mice. We considered that a search was made when a mouse poked its nose into or placed its head over the hole. Measurements of the time spent in the maze, the number of searches over non-target holes and the distance traveled before finding the target hole were made. Although acquisition training was started with 12 *Scn1a*$^{+/+}$ mice and 12 *Scn1a*$^{RX/+}$ mice each, the final analysis included 11 *Scn1a*$^{+/+}$ mice and 11 *Scn1a*$^{RX/+}$ mice. We excluded one *Scn1a*$^{+/+}$ mouse from the analysis because this mouse seemed to find the target hole but avoided entering straight into the escape box in some acquisition training trials, for an unknown reason. This mouse was detected as an outlier by Grubbs' test at the 1% significance level. We also excluded one Scn1a$^{RX/+}$ mouse from the analysis because this mouse jumped out of the maze before finding the target hole and failed to complete the trial. On day 5, a probe test was conducted for 3 min without the escape box to confirm that this spatial task was carried out through navigation using distal environment room cues. The numbers of searches over each hole were counted. On days 8–11 (reversal days r1–r4), reversal training took place. During reversal training, the escape box was placed underneath the hole opposite the old target hole that had been used during acquisition training. Measurements of the time spent in the maze, the number of searches over the old target hole, the number of searches of non-target holes and the distance traveled before finding the novel target hole were made. On day 12, a probe test was conducted for 3 min without the escape box. We excluded two *Scn1a*$^{RX/+}$ mice from the analysis because they jumped out of the maze before they completed the probe test. The numbers of searches over each hole were counted.

Light/dark box test

The light/dark box consisted of two equal-sized plastic boxes (20×20×20 cm) connected by a shuttle door (3×5 cm) located in the center of the partition (O'Hara & Co.). A 23-week-old male mouse was placed on the light side of the apparatus and allowed to explore the boxes freely for 5 min; activities were analyzed using Image J EP software (O'Hara & Co.). Measurements of time spent and distance traveled in each side were made.

Free-moving social test

Two mice, which had previously been housed in different cages, were placed into an open field (40×40×30 cm) with food and water available ad libitum and allowed to explore the field freely for 6 h with video recording. The number of physical contacts between the two mice was counted during the session time using Image J OF software (O'Hara & Co.). The number of nose-to-nose contacts and physical contacts between the two mice for 20 min, after the habituation period of 10 min, was also analyzed. This test was performed with 27- to 28-week-old *Scn1a*$^{+/+}$ and *Scn1a*$^{RX/+}$ male mice (n=12, each group). Furthermore, the number of nose-to-nose contacts and physical contacts between pairs of adult *Scn1a*$^{+/+}$ mice and a C57BL/6J juvenile and pairs of adult *Scn1a*$^{RX/+}$ mice and a C57BL/6J juvenile was counted.

Buried food test

The buried food test was performed as previously described (Yang and Crawley, 2009). 15- to 16-week-old male mice were food-deprived for 16 h with access to water ad libitum. Each mouse was placed in the cage containing about 3 cm of clean virgin pulp paper chip bedding (Alpha-Dri, Shepherd Specialty Products, Kalamazoo, MI), and allowed to explore the entire test cage for 5 min for habituation. A small piece of cookie was then buried approximately 1 cm beneath the surface on a corner location of the cage, and the latency to find the food was measured in seconds up to a maximum of 900 s. We defined finding the food as when the mouse started eating or holding the food with their forepaws. For the mice which failed to find the buried food after 15 min have elapsed, 900 s was recorded. The site of mouse placement and the site at which the food was buried were always the same. N13 *Scn1a*$^{RX/+}$ male mice and age-matched *Scn1a*$^{+/+}$ male littermates (n=11, each group) were tested.

Rotarod test

The rotarod test was performed as described previously (Carter et al., 2001), with minor modifications. Briefly, the rotarod apparatus consisted of a gridded plastic rod (3-cm in diameter) (Muromachi Kikai, Tokyo, Japan). On the first day (day 1), 7- to 8-week-old male mice were given a training session, during which each mouse was placed on the rotarod at a constant speed (4 rpm) for 180 s. Afterwards, mice received one trial per day during 4 consecutive days (days 1 to 4). During each test session, each mouse was placed on the rod rotating at a constant speed (4 rpm) for 60 s for habituation, and then the rotarod was accelerated from 4 to 40 rpm over 300 s. The latency to fall off the rotarod was recorded. For the mice which stayed on the rotarod during 300 s, 300 s was recorded. N14 *Scn1a*$^{RX/+}$ male mice and age-matched *Scn1a*$^{+/+}$ male littermates (n=8, each group) were tested.

Footprint test

The footprint test was performed as described previously (Carter et al., 2001), with slight modifications. Briefly, the apparatus was a narrow, open-top runway (60×5×10 cm). The forepaws and hindpaws of 9-week-old male mice were coated with black and red paints, respectively, and the mice were allowed to walk down the runway covered with white paper. The footprint patterns were assessed quantitatively by four measurements including stride length, hindbase width, frontbase width, and front/hind footprint overlap. Stride length was measured as the average distance of forward movement between each stride. Hind-base width and front-base width were measured as the average distance between left and right hind footprints and left and right front footprints, respectively. Distance from left or right front footprint/hind footprint overlap was used to measure uniformity of step alternation. When the center of the hind footprint fell on top of the center of the preceding front footprint, a value of zero was recorded. When the footprints did not overlap, the distance between the center points of the footprints was recorded. N14 *Scn1a*$^{RX/+}$ male mice and age-matched *Scn1a*$^{+/+}$ male littermates (n=8, each group), which were subjected the rotarod test a week ago, were examined.

Electroencephalography (EEG) recordings

Stainless steel monopolar electrodes were guided into the cortex (from Bregma, anterior–posterior, 1.0 mm; medial–lateral, 1.0 mm; ventral, 0.7 mm) and the hippocampus (from Bregma, anterior–posterior, 2.2 mm; medial–lateral, 2.0 mm; ventral, 1.2 mm) under 1.5% halothane anesthesia with N_2O:O_2 (1:1) ventilation. A reference electrode was implanted in the cerebellum (at midline, 2.0 mm posterior to lambda). At least one week after surgery, EEG recordings were continuously taken for 6 h (3 h each in the day time, 17:00 to 20:00, and night time, 20:00 to 23:00). The data were analyzed using SleepSign software (KISSEI COMTEC, Nagano, Japan). The power spectrum of the frequency bands (0.5–100 Hz) in EEG recordings was analyzed using fast Fourier transform analysis. Three stages including waking, slow-wave sleep and rapid eye movement (REM) sleep stages were scored for every 4-second epoch, as determined by visual inspection of the EEG and EMG records. Epochs containing EEG artifacts were excluded from

spectral analysis. EEG recordings were performed using 28- to 35-week-old *Scn1a*$^{+/+}$ and *Scn1a*$^{RX/+}$ male mice (n = 4, each group).

Statistical analyses

Comparisons between *Scn1a*$^{+/+}$ and *Scn1a*$^{RX/+}$ mice were performed using Mann–Whitney *U* tests. Dependent variables were analyzed by analysis of variance (ANOVA). Comparisons within each genotype were performed using paired *t*-tests. Grubbs' test was used to detect outliers. Values with $p<0.05$ were considered to be significant.

Results

Scn1a$^{RX/+}$ *mice in home cages show reduced spontaneous motor activity and enhanced grooming*

We previously reported that a subpopulation of *Scn1a*$^{RX/+}$ mice show recurrent spontaneous seizures after P18 (Ogiwara et al., 2007). However in the present study we employed mice that showed no seizures at least during the behavioral tests. We first assessed the spontaneous home cage activity of *Scn1a*$^{RX/+}$ male mice. In terms of locomotion, while distance traveled per hour was shorter in *Scn1a*$^{RX/+}$ mice than in *Scn1a*$^{+/+}$ mice (Fig. 1A), the percentage of time spent walking was insignificantly reduced in *Scn1a*$^{RX/+}$ mice compared with control *Scn1a*$^{+/+}$ littermates (Fig. 1B). We divided walking into three subclasses including walking fast (or walking in a definite direction), walking slowly and turning, and found that the percentage of time spent walking fast was significantly smaller in *Scn1a*$^{RX/+}$ mice than in *Scn1a*$^{+/+}$ mice (Fig. 1C). The percentage of time spent performing other walking subtypes did not differ significantly between the genotypes (data not shown). The spontaneous home cage activity test also showed that the percentage of time spent rearing was decreased in *Scn1a*$^{RX/+}$ mice compared with *Scn1a*$^{+/+}$ mice (Fig. 1D). Altogether, these results suggested that *Scn1a*$^{RX/+}$ mice had reduced spontaneous motor activity in their home cages.

Scn1a$^{RX/+}$ mice were heavier than *Scn1a*$^{+/+}$ mice at the time of the home cage spontaneous activity test (8 to 10-week-old: 25.7 ± 0.58 g (means ± SEM) for *Scn1a*$^{+/+}$; 28.9 ± 0.96 g for *Scn1a*$^{RX/+}$; Mann–Whitney *U* test; $p<0.01$). The increased body weight in *Scn1a*$^{RX/+}$ mice can be related to reduced spontaneous motor activity in the home cages.

The percentage of time spent grooming, which is thought to correspond to stereotypy in autism spectrum disorders (ASDs) (McFarlane et al., 2008), was increased in *Scn1a*$^{RX/+}$ mice compared with *Scn1a*$^{+/+}$ mice (Fig. 1E). The number of grooming bouts per hour was also increased in *Scn1a*$^{RX/+}$ mice compared with *Scn1a*$^{+/+}$ mice (Fig. 1F). Enhanced grooming in *Scn1a*$^{RX/+}$ mice might be analogous to the gestural stereotypy in Dravet syndrome patients (Dravet et al., 2005).

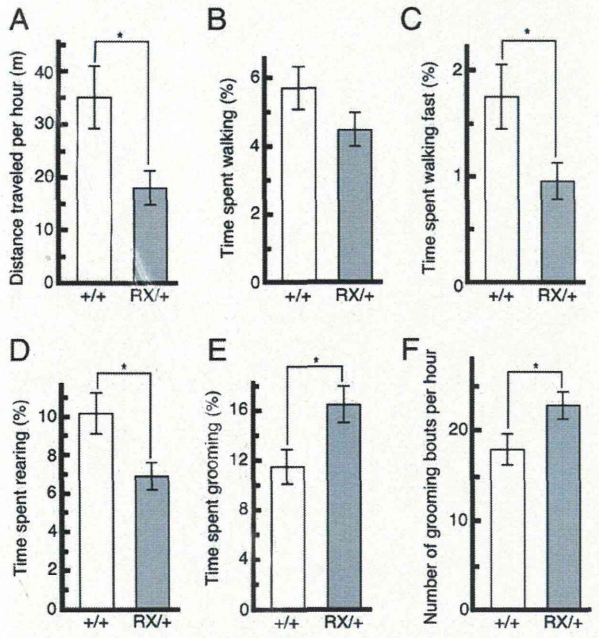

Fig. 1. *Scn1a*$^{RX/+}$ mice show altered spontaneous home cage activity. (A) Distance traveled per hour was reduced in *Scn1a*$^{RX/+}$ mice compared with *Scn1a*$^{+/+}$ mice (Mann–Whitney *U* test; $p<0.05$). (B) The percentage of time spent walking did not differ between *Scn1a*$^{+/+}$ and *Scn1a*$^{RX/+}$ mice (Mann–Whitney *U* test; p = ns (not significant)). (C) The percentage of time spent walking fast was decreased in *Scn1a*$^{RX/+}$ mice compared with *Scn1a*$^{+/+}$ mice (Mann–Whitney *U* test; $p<0.05$). (D) The percentage of time spent rearing was decreased in *Scn1a*$^{RX/+}$ mice compared with that in *Scn1a*$^{+/+}$ mice (Mann–Whitney *U* test; $p<0.05$). (E) The percentage of time spent grooming was increased in *Scn1a*$^{RX/+}$ mice compared with that in *Scn1a*$^{+/+}$ mice (Mann–Whitney *U* test; $p<0.05$). For hanging, eating, drinking, resting and micromovements, there were no significant differences between the genotypes (data not shown). (F) The number of grooming bouts per hour was increased in *Scn1a*$^{RX/+}$ mice compared with *Scn1a*$^{+/+}$ mice (Mann–Whitney *U* test; $p<0.05$). The white and grey bars represent *Scn1a*$^{+/+}$ and *Scn1a*$^{RX/+}$ mice, respectively (n = 12, each group). Data represent means ± SEM, *$p<0.05$.

Scn1a$^{RX/+}$ *mice in novel environments are hyperactive*

We next assessed the novelty-induced locomotor activity and anxiety-like behavior of *Scn1a*$^{RX/+}$ male mice that had been transferred from familiar home cages to a novel open field. In the first 10-minute session, total distance traveled was longer in *Scn1a*$^{RX/+}$ mice than in control *Scn1a*$^{+/+}$ littermates (Fig. 2A), suggesting that *Scn1a*$^{RX/+}$ mice were hyperactive. Total distance traveled of *Scn1a*$^{RX/+}$ mice was gradually reduced during a period of 30 min and reached a similar level to that of *Scn1a*$^{+/+}$ mice in the last session. These results suggested that *Scn1a*$^{RX/+}$ mice had a novelty/novel environment-induced locomotor hyperactivity, which might be analogous to the hyperactivity seen in Dravet syndrome patients (Dravet et al., 2005).

The length of time spent in the center of the open field, which can be thought to correlate inversely with the anxiety level of an animal, was also analyzed (Fig. 2B). In *Scn1a*$^{+/+}$ mice, the length of time spent in the center of the open field gradually increased during a period of 30 min. However, in *Scn1a*$^{RX/+}$ mice, the length of time spent in the center of the open field remained low during a 30-minute period. An ordinal explanation of this observation would be that *Scn1a*$^{RX/+}$ mice maintain anxiety at a high level for at least 30 min.

We then assessed the novelty-induced locomotion and anxiety-like behavior of *Scn1a*$^{RX/+}$ male mice using the elevated-plus maze test, which exploits the conflict between exploration of a novel area and aversion to open areas. In the maze, *Scn1a*$^{RX/+}$ mice traveled over a greater total distance than *Scn1a*$^{+/+}$ mice (Fig. 2C), consistent with the novelty-induced locomotor hyperactivity observed in the previous open field test. *Scn1a*$^{RX/+}$ mice also exhibited an increased percentage of time spent in the open arms and an increased number of entries into open arms (Figs. 2D, E), suggesting that *Scn1a*$^{RX/+}$ mice had a lowered level of anxiety-like behavior. However, they showed increased anxiety-like behavior in the previous novel open field test. This inconsistency will be discussed later (see Discussion).

We also investigated the novelty-induced locomotion and anxiety-like behavior of *Scn1a*$^{RX/+}$ male mice using the light/dark box test. *Scn1a*$^{RX/+}$ mice showed increased total distance traveled and total number of transitions between the light and dark sides compared with *Scn1a*$^{+/+}$ mice (Figs. 2F, G), consistent with novelty-induced locomotor hyperactivity. The length of time spent in the dark side was similar between *Scn1a*$^{RX/+}$ and *Scn1a*$^{+/+}$ mice (Fig. 2H), suggesting that *Scn1a*$^{RX/+}$ mice had a normal level of light/dark preference.

Scn1a$^{RX/+}$ *mice show lowered sociability*

Most Dravet syndrome patients have poor social relationships (Caraballo and Fejerman, 2006; Cassé-Perrot et al., 2001; Dravet et al.,

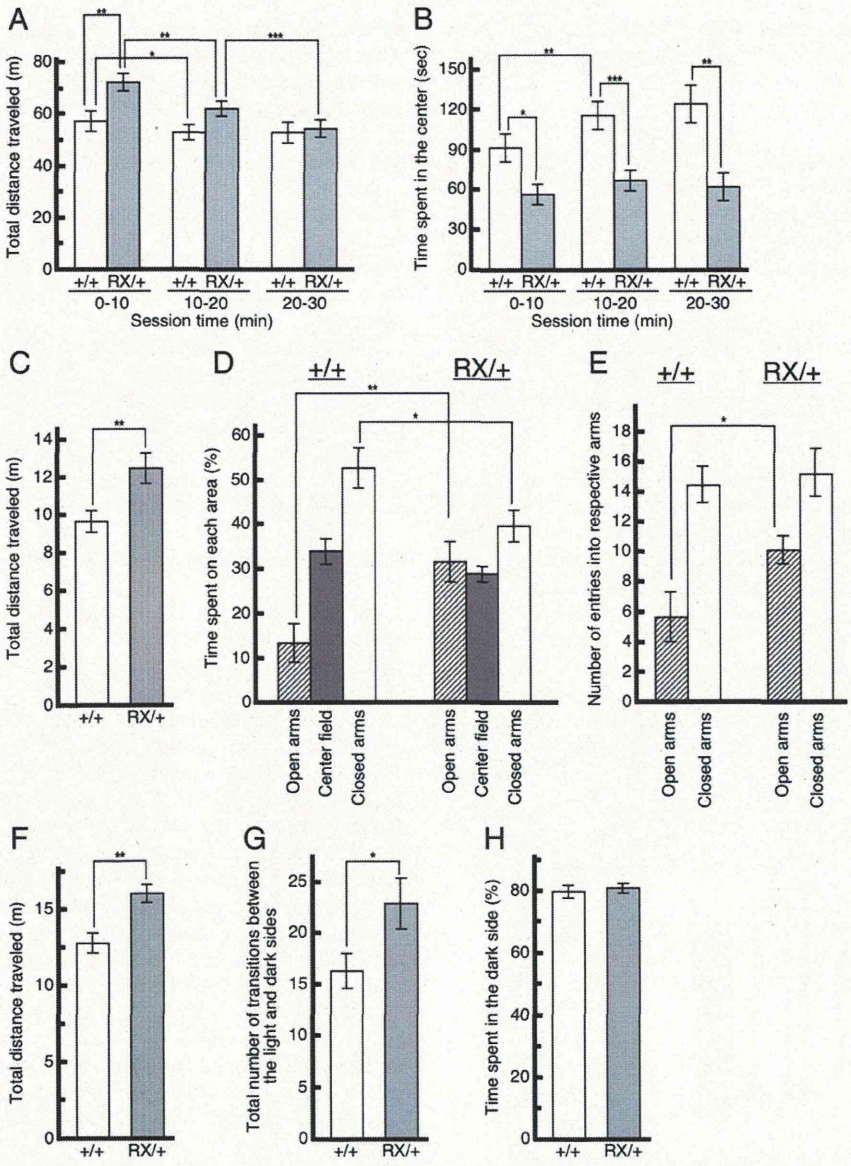

Fig. 2. *Scn1a*$^{RX/+}$ mice show increased locomotor activity and altered anxiety-like behaviors in novel environments. (A,B) Results in the open field test. (A) The total distance traveled in the first 10-minute session was larger in *Scn1a*$^{RX/+}$ mice than in *Scn1a*$^{+/+}$ mice (Mann–Whitney *U* test; $p<0.01$). The total distance traveled in the second and third 10-minute sessions was similar between *Scn1a*$^{RX/+}$ mice and *Scn1a*$^{+/+}$ mice (repeated measures ANOVA; main effect genotype: $F(1, 22)=3.7$, $p=$ ns; main effect time: $F(2, 44)=20.9$, $p<0.001$; interaction: $F(2, 44)=7.2$, $p<0.01$: Mann–Whitney *U* test; $p=$ ns). While the total distance traveled by *Scn1a*$^{+/+}$ mice was reduced between the first and second sessions (paired *t*-test; first session vs. second session: $p<0.05$), the total distance traveled by *Scn1a*$^{RX/+}$ mice was gradually reduced during a 30-minute period (paired *t*-test; first session vs. second session: $p<0.01$; second session vs. third session: $p<0.001$). (B) The length of time spent in the center of the open field was shorter in *Scn1a*$^{RX/+}$ mice than in *Scn1a*$^{+/+}$ mice during a 30-minute period (repeated measures ANOVA; main effect genotype: $F(1, 22)=18.6$, $p<0.001$; main effect time: $F(2, 44)=4.1$, $p=$ ns; interaction: $F(2, 44)=1.6$, $p=$ ns; Mann–Whitney *U* test; first session: $p<0.01$; second session: $p<0.01$; third session: $p<0.01$). While the length of time spent in the center of the open field by *Scn1a*$^{+/+}$ mice was increased between the first and second sessions (paired *t*-test; $p<0.05$), the length of time spent in the center of the open field by *Scn1a*$^{RX/+}$ mice remained low during a 30-minute period (paired *t*-test; $p=$ ns). The white and grey bars represent *Scn1a*$^{+/+}$ and *Scn1a*$^{RX/+}$ mice, respectively ($n=12$, each group). (C–E) Results in the elevated-plus maze test. (C) The total distance traveled by *Scn1a*$^{RX/+}$ mice was greater than that traveled by *Scn1a*$^{+/+}$ mice (Mann–Whitney *U* test; $p<0.01$). The white and grey bars represent *Scn1a*$^{+/+}$ and *Scn1a*$^{RX/+}$ mice, respectively ($n=12$, each group). (D) The percentage of time spent in open arms was higher in *Scn1a*$^{RX/+}$ mice than in *Scn1a*$^{+/+}$ mice (Mann–Whitney *U* test; $p<0.01$). In contrast, the percentage of time spent in closed arms was smaller in *Scn1a*$^{RX/+}$ mice than in *Scn1a*$^{+/+}$ mice (Mann–Whitney *U* test; $p<0.05$). (E) The total number of entries into open arms was higher in *Scn1a*$^{RX/+}$ mice than in *Scn1a*$^{+/+}$ mice (Mann–Whitney *U* test; $p<0.05$). The hatched, grey and white bars in (D,E) represent the open arms, center field and closed arms, respectively. (F–H) Results in the light/dark box test. (F) The total distance traveled was greater in *Scn1a*$^{RX/+}$ mice than *Scn1a*$^{+/+}$ mice (Mann–Whitney *U* test; $p<0.01$). (G) The total number of transitions between light and dark sides was higher in *Scn1a*$^{RX/+}$ mice than in *Scn1a*$^{+/+}$ mice (Mann–Whitney *U* test; $p<0.05$). (H) The percentage of time spent in the dark side was similar in *Scn1a*$^{RX/+}$ and *Scn1a*$^{+/+}$ mice (Mann–Whitney *U* test; $p=$ ns). The white and grey bars represent *Scn1a*$^{+/+}$ and *Scn1a*$^{RX/+}$ mice, respectively ($n=12$, each group). Data represent means ± SEM, $^{*}p<0.05$, $^{**}p<0.01$, $^{***}p<0.001$.

2005; Nolan et al., 2006; Ragona et al., 2010; Wolff et al., 2006). We assessed whether *Scn1a*$^{RX/+}$ male mice have altered social behavior using the three-chambered social interaction test (Moy et al., 2007; Silverman et al., 2010). In the test that quantifies the preference of a mouse for a novel unfamiliar mouse (stranger 1) versus an empty wire cage, control *Scn1a*$^{+/+}$ littermates apparently preferred stranger 1 to the empty cage, whereas *Scn1a*$^{RX/+}$ mice showed equal preferences for the enclosed stranger 1 and the empty cage (Fig. 3A). Because the sociability level can be reflected in the length of time spent in the chamber with the unfamiliar mouse (stranger 1), these observations suggested that *Scn1a*$^{RX/+}$ mice had a lowered level of sociability. The impaired sociability of *Scn1a*$^{RX/+}$ mice was further supported by the observations

that, while *Scn1a*$^{+/+}$ mice spent more time sniffing stranger 1 than the empty cage, *Scn1a*$^{RX/+}$ mice spent similar amounts of time sniffing stranger 1 and the empty cage (Fig. 3B).

We next tested preference for social novelty using a test that quantifies the preference of a mouse for a novel unfamiliar stranger 2 mouse versus the stranger 1 mouse placed in the previous test

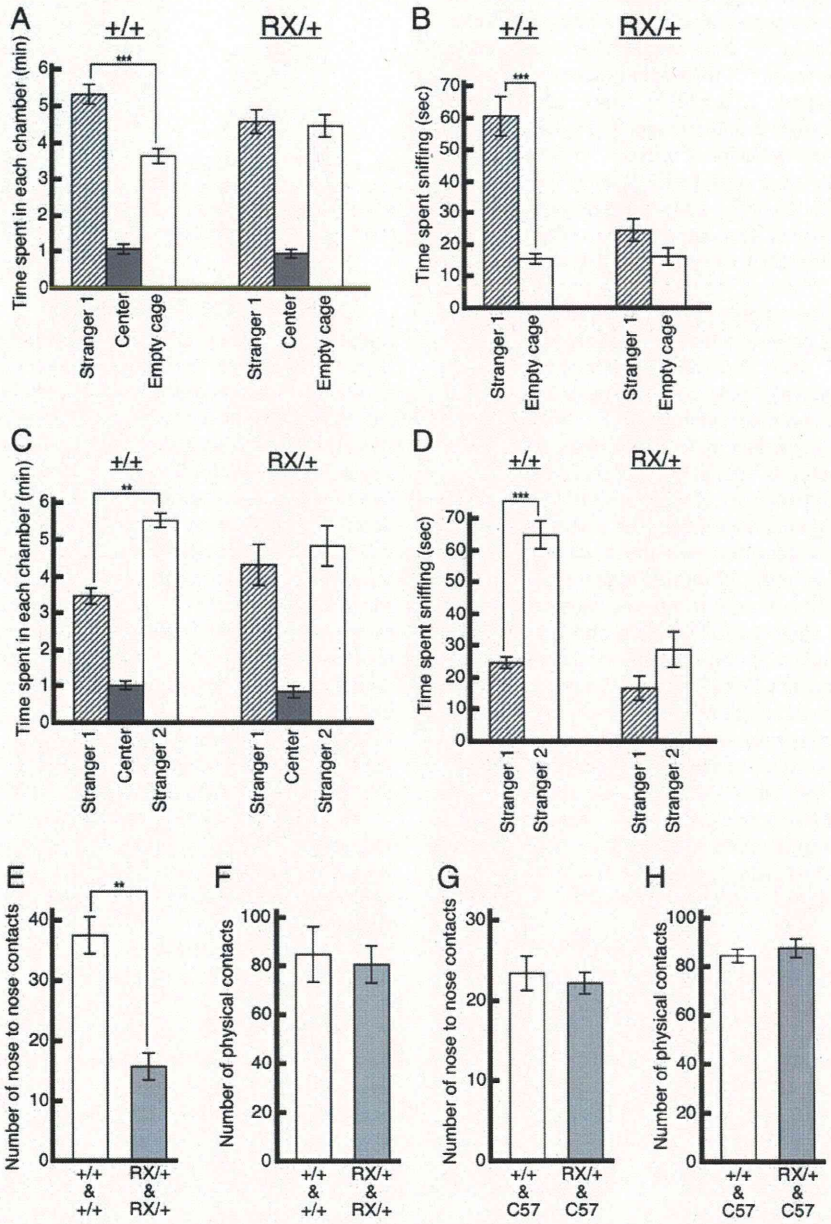

Fig. 3. *Scn1a*$^{RX/+}$ mice show impaired social behaviors in the social tests. (A,B) Results of the test for sociability in the three-chambered social interaction test. (A) Duration of time spent in chambers with and without stranger mice. While *Scn1a*$^{+/+}$ mice spent more time in the chamber containing stranger 1 than in the chamber containing the empty cage (paired *t*-test; $p<0.01$), *Scn1a*$^{RX/+}$ mice showed no preference for chambers with or without strangers (paired *t*-test; p = ns). (B) Duration of time spent sniffing a new stranger 1 mouse and the empty cage. While *Scn1a*$^{+/+}$ mice spent more time sniffing the cage containing new stranger 1 than the empty cage (paired *t*-test; $p<0.001$), *Scn1a*$^{RX/+}$ mice showed no preference for cages with or without strangers (paired *t*-test; p = ns). (C,D) Results of the test for preference for social novelty in the three-chambered social interaction test. (C) Duration of time spent in chambers with the familiarized stranger 1 mouse and a new stranger 2 mouse. While *Scn1a*$^{+/+}$ mice spent more time in the chamber containing stranger 2 than in the chamber containing stranger 1 (paired *t*-test; $p<0.01$), *Scn1a*$^{RX/+}$ mice showed no preference for either chamber (paired *t*-test; p = ns). (D) Duration of time spent sniffing the familiarized stranger 1 mouse and a new stranger 2 mouse. While *Scn1a*$^{+/+}$ mice spent more time sniffing the cage containing new stranger 2 than that containing the familiarized stranger 1 (paired *t*-test; $p<0.001$), *Scn1a*$^{RX/+}$ mice showed no preference for either cage (paired *t*-test; p = ns). The hatched, grey and white bars represent the side chamber with stranger 1, the center chamber and the chamber without a stranger or with stranger 2, respectively. n = 12, each group. (E,F) *Scn1a*$^{RX/+}$ mice show lowered sniffing behaviors in an open field in which two mice move freely. (E) The total number of nose-to-nose contacts for 20 min, after habituation periods of 10 min, was smaller in *Scn1a*$^{+/+}$ pairs of the same age than in age-matched *Scn1a*$^{RX/+}$ pairs of same age (Mann–Whitney *U* test; $p<0.01$; n = 6, each group). (F) The total number of physical contacts, including both social and non-social interactions, was similar in *Scn1a*$^{+/+}$ pairs of same age and *Scn1a*$^{RX/+}$ pairs of same age (Mann–Whitney *U* test; p = ns). The white bars represent the pairs of *Scn1a*$^{+/+}$ mice. The grey bars represent the pairs of *Scn1a*$^{RX/+}$ mice. (G,H) *Scn1a*$^{RX/+}$ male mice toward actively-approaching unfamiliar juveniles showed normal levels of social behaviors. (G) The total number of nose-to-nose contacts for 20 min, after habituation periods of 10 min, was similar between pairs of adult *Scn1a*$^{+/+}$ mice and a C57BL/6J juvenile and pairs of adult *Scn1a*$^{RX/+}$ mice and a C57BL/6J juvenile (Mann–Whitney *U* test; p = ns; n = 12, each group). (H) The total number of physical contacts was similar between pairs of adult *Scn1a*$^{+/+}$ mice and a C57BL/6J juvenile and pairs of adult *Scn1a*$^{RX/+}$ mice and a C57BL/6J juvenile (Mann–Whitney *U* test; p = ns). The white and grey bars represent paired *Scn1a*$^{+/+}$ mice with a C57BL/6J mouse and paired *Scn1a*$^{RX/+}$ mice with a C57BL/6J mouse. Data represent means ± SEM, $^{**}p<0.01$, $^{***}p0.001$.

(Fig. 3C). While control *Scn1a*$^{+/+}$ littermates preferred novel stranger 2 to stranger 1, *Scn1a*$^{RX/+}$ mice showed equal preferences for novel stranger 2 and stranger 1. Because the preference level can be judged from the length of time spent in the chamber with the novel mouse (stranger 2), these observations suggested that *Scn1a*$^{RX/+}$ mice had a lower level of preference for social novelty. This impaired preference for social novelty in *Scn1a*$^{RX/+}$ mice was further supported by the observations that, while *Scn1a*$^{+/+}$ mice spent more time sniffing novel stranger 2 than stranger 1, *Scn1a*$^{RX/+}$ mice spent similar amounts of time sniffing stranger 2 and stranger 1 (Fig. 3D).

We then investigated social behavior of *Scn1a*$^{RX/+}$ mice under the condition in which two male mice were freely moving (Silverman et al., 2010). As shown in Fig. 3E, *Scn1a*$^{RX/+}$ pairs of the same age showed a reduced total number of nose-to-nose contacts compared with age-matched *Scn1a*$^{+/+}$ control pairs, consistent with lowered levels of sniffing behavior of *Scn1a*$^{RX/+}$ mice in the three-chambered interaction social test. We also counted the number of physical contacts. As shown in Fig. 3F, the total number of physical contacts was similar in *Scn1a*$^{RX/+}$ pairs and control *Scn1a*$^{+/+}$ pairs, and was not different during the session for 6 h (data not shown). These observations suggested that, despite a reduced social approach behavior, *Scn1a*$^{RX/+}$ mice preferred to be together with partners, possibly due to their desire for physical comfort (thermal comfort, softness, etc.) but not for social relations.

We also investigated the behaviors of adult *Scn1a*$^{RX/+}$ male mice toward actively-approaching unfamiliar mice. The partner mice used in the test were C57BL/6J juveniles that were much younger than the *Scn1a*$^{RX/+}$ mice to exclude an effect of mutual aggression. As shown in Figs. 3G, H, the total numbers of nose-to-nose contacts and physical contacts between pairs of adult *Scn1a*$^{RX/+}$ mice and an unfamiliar C57BL/6J juvenile were similar to those between control pairs of *Scn1a*$^{+/+}$ mice and an unfamiliar C57BL/6J juvenile. These observations suggested that *Scn1a*$^{RX/+}$ mice did not reject the active approaches of C57BL/6J juvenile and had good relationships with the mice.

Taken together, these results of social tests showed that *Scn1a*$^{RX/+}$ mice had impaired social behaviors, which was pronounced when their partner mice did not make active approaches. This altered social behavior might be relevant to the poor social relationships of Dravet syndrome (Caraballo and Fejerman, 2006; Cassé-Perrot et al., 2001; Dravet et al., 2005; Nolan et al., 2006; Ragona et al., 2010; Wolff et al., 2006).

Although *Scn1a*$^{RX/+}$ mice were heavier than *Scn1a*$^{+/+}$ mice at the time of the three-chambered social interaction test (17-week-old: 28.4 ± 0.45 g for *Scn1a*$^{+/+}$ mice; 31.4 ± 1.30 g for *Scn1a*$^{RX/+}$ mice; Mann–Whitney U test; $p<0.05$), the body weight was similar between genotypes at the time of the free-moving social test (28–29-weeks old: 36.6 ± 0.74 g for *Scn1a*$^{+/+}$ mice; 39.8 ± 2.23 g for *Scn1a*$^{RX/+}$ mice; Mann–Whitney *U* test; p = ns (not significant)). The body weights therefore did not seem to be a major factor contributing to impaired social behaviors of *Scn1a*$^{RX/+}$ mice.

Scn1a$^{RX/+}$ mice may have an olfaction defect

Because *Scn1a*$^{RX/+}$ male mice showed lowered levels of sniffing behavior in the social tests described above, we examined their olfactory ability using the buried food test. As shown in Fig. 4, latency to find the buried food was longer in *Scn1a*$^{RX/+}$ mice than in *Scn1a*$^{+/+}$ control littermates, suggesting that *Scn1a*$^{RX/+}$ mice might have poor ability to smell and it might have partially contributed to the above-mentioned impaired sniffing behavior of the mice.

Scn1a$^{RX/+}$ mice have lowered spatial and reversal task learning ability

Because visuo-perceptual skills are impaired in Dravet syndrome patients (Cassé-Perrot et al., 2001; Chieffo et al., 2011; Dravet et al., 2005; Wolff et al., 2006), we assessed spatial learning ability of *Scn1a*$^{RX/+}$ male mice using the Barnes maze test (Pompl et al., 1999). Over the course of 4 days of acquisition training trials (acquisition days a1–a4) (Figs. 5A–C), control *Scn1a*$^{+/+}$ littermates exhibited progressive reductions in the numbers of searches over non-target holes, distance traveled and time spent in the maze, suggesting that control *Scn1a*$^{+/+}$ mice steadily learned to navigate to the target hole on the basis of the available visual cues. In trials for *Scn1a*$^{RX/+}$ mice, the number of searches over the non-target holes, distance traveled and time spent on the maze were reduced from day a1 to day a2 (Figs. 5A–C). However, the number of searches over non-target holes, distance traveled and time spent on the maze were not improved from day a2 to day a3 or from day a3 to day a4. In addition, *Scn1a*$^{RX/+}$ mice exhibited higher numbers of searches over non-target holes and longer distance traveled than *Scn1a*$^{+/+}$ mice on days a3 and a4 (Figs. 5A, B). Furthermore, although *Scn1a*$^{RX/+}$ mice found the target hole faster than *Scn1a*$^{+/+}$ mice on days a1 and a2 possibly due to their novelty-induced locomotor hyperactivity, *Scn1a*$^{RX/+}$ mice found the target hole slower than *Scn1a*$^{+/+}$ mice on day a4 (Fig. 5C). These observations suggested that *Scn1a*$^{RX/+}$ mice are poorer at learning the target hole location than *Scn1a*$^{+/+}$ mice.

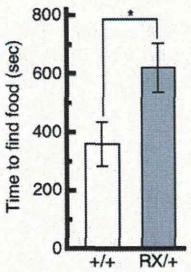

Fig. 4. *Scn1a*$^{RX/+}$ mice have olfactory impairment in the buried food test. *Scn1a*$^{RX/+}$ mice took a longer time to find the buried food than *Scn1a*$^{+/+}$ mice (Mann–Whitney *U* test; $p<0.05$). The white and grey bars represent *Scn1a*$^{+/+}$ and *Scn1a*$^{RX/+}$ mice, respectively (n = 11, each group). Data represent means ± SEM, *$p<0.05$.

In the probe test after acquisition training (Fig. 5D), while *Scn1a*$^{+/+}$ mice predominantly preferred the target hole to adjacent non-target holes, *Scn1a*$^{RX/+}$ mice did not show such a strong preference, providing additional evidence suggesting that *Scn1a*$^{RX/+}$ mice have lowered spatial learning ability.

We next assessed the reversal task learning ability of *Scn1a*$^{RX/+}$ mice by moving the target hole to the opposite side of the Barnes maze (Nakatani et al., 2009) (Fig. 6). Over the course of 4 days of reversal training trials (reversal days r1–r4) (Figs. 6A–C), *Scn1a*$^{+/+}$ mice exhibited progressive reductions in the numbers of searches over non-target holes, distance traveled and time spent in the maze, suggesting that *Scn1a*$^{+/+}$ mice steadily learned the novel target hole location. *Scn1a*$^{RX/+}$ mice also progressively reduced the numbers of searches over non-target holes, distance traveled and time spent in the maze over the course of training trials, suggesting that *Scn1a*$^{RX/+}$ mice steadily learned the novel target hole location. However, *Scn1a*$^{RX/+}$ mice exhibited higher numbers of searches over non-target holes than *Scn1a*$^{+/+}$ mice on days r2, r3 and r4 (Fig. 6A). Similarly, *Scn1a*$^{RX/+}$ mice traveled further than *Scn1a*$^{+/+}$ mice on days r3 and r4 (Fig. 6B). These observations suggested that *Scn1a*$^{RX/+}$ mice were poor at learning the novel target hole location compared with *Scn1a*$^{+/+}$ mice.

A lowered level of reversal task learning could occur as a result of a spatial learning disability or inflexibility to environmental change. To investigate the flexibility of *Scn1a*$^{RX/+}$ mice to a maze with a novel target hole location, we analyzed the number of searches over the old target hole. As shown in Fig. 6D, *Scn1a*$^{+/+}$ mice progressively reduced the number of searches over the old target hole over the course of reversal training trials, suggesting that *Scn1a*$^{+/+}$ mice were well familiarized with the maze with the novel target hole location. Like *Scn1a*$^{+/+}$ mice, *Scn1a*$^{RX/+}$ mice exhibited progressive reduction in the number of searches over the old target hole over the course of